Riyah N. Kiter
College of Engineering,
University of Anbar, Iraq
riyahnajim@hotmail.com

Received on: 11/04/2017
Accepted on: 17/08/2017

Proposed Design Against High-Cycle Fatigue Failure of Metallic Beams Using Lamination

Abstract-*Fatigue analysis helps in predicting life of the component and seeks improvements of the whole process in design phase. Efforts are continually made to combat the fatigue phenomenon, yet certain mechanical components are still failing due to fatigue. The present work proposes a laminated design of beams, which undergo fatigue. The well-known Paris-Erdogan formula was used to theoretically predict fatigue life of the proposed design. The design was shown to enhance fatigue properties through laminating the cross section of the component; Barriers in front of a propagating crack is deliberately included by lamination. Spectacular levels of improvement in the fatigue life of up to 102% were achieved by replacing the monolithic type by only seven laminates. The present analysis was proved efficient in verifying the anticipated improvement acquired by the proposed design of laminated beams.*

Keywords: *Fatigue, lamination, life prediction, design, beam, Paris-Erdogan.*

How to cite this article: R.N. Kiter, "Proposed Design Against High-Cycle Fatigue Failure of Metallic Beams Using Lamination" *Engineering and Technology Journal*, Vol. 36, Part A, No. 5, pp. 574-581, 2018.

1. Introduction

Fatigue has been traditionally described as the progressive localized irreversible damage that occurs in a material subjected to repeated or fluctuating stresses usually of values less than the tensile strength and even less than the yield strength of that material. Fracture of components due to fatigue is the most common cause of failure in service, especially in shafts and axles, springs, aircraft wings, pressure vessels etc., where loading stresses are fluctuating about some mean values. Fatigue failure begins when a crack is initiated from points of high stress concentration on the surface of the component and then propagates under the effect of the load cycles until it reaches a critical size when the remaining cross-section can no longer sustain the load and fast fracture takes place. Even in the absence of such points of high stress concentration, fatigue can usually onset by the action of characteristic slip band accumulation on the surface of the specimen. Various conditions, that can accelerate crack initiation and rate and direction of crack propagation, include residual tensile stresses, elevated temperatures, temperature cycling, a corrosive environment, and high-frequency cycling. Initially the cracks will form in the surface grains and develop along the active slip plane aligned with the direction of maximum shear within the component, i.e. at 45^0 to the maximum tensile stress; this is often referred to as StageI growth and is favored by zero mean stress and low cyclic stress conditions. At some point, usually when the crack encounters a grain boundary, StageI is replaced by StageII growth in which the crack is normal to the maximum principal tensile stress; this stage is favored by a tensile mean stress and high cyclic stress conditions. Once the fatigue crack has reached some critical length such that the energy for further growth can be obtained from the elastic energy of the surrounding metal, catastrophic failure takes place; this stage is denoted by StageIII [1-7].

2. Relevant Literature

Although fatigue analysis helps in predicting life of the component, it can aid to seek improvements of the whole process in design phase itself. For many decades, efforts are continually made to combat the fatigue phenomenon, yet certain mechanical components are still failing due to fatigue. Proper design against fatigue behavior with generous factors of safety were the backbone of modern task made by many researchers to obstacle the frequent occurrence of catastrophic failures associated with fatigue. For one example of the efforts made to improve the fatigue characteristics, the effect of layering a cold rolled sheet of mild steel with composite coatings was examined by Kovarika et al. [1]. Plain substrates, grit-blasted substrates, and plasma sprayed specimens with one to three layers of coating were studied. The layered coatings were composed of alternating sequence of ceramic (Cr_2O_3) and metallic (Ni10wt%Al) layers. Although grit blasting did not influence fatigue life of substrate, the Cr_2O_3 deposit leads to a fatigue life increase due to compressive residual stress field present in substrate below the Cr_2O_3

https://doi.org/10.30684/etj.36.5A.13
2412-0758/University of Technology-Iraq, Baghdad, Iraq

layer. Moreover, the Ni10wt%Al coatings decreased fatigue life because the compressive stress was reduced in substrate in addition to the increased number of fatigue cracks and their localization. The aim of mechanical improvement of fatigue life was usually related to the accuracy of fatigue life prediction. Too many attempts were made to establish an acceptable method to accurately predict fatigue lives. Fatigue life prediction techniques were reviewed and analyzed by Fleck and Smith [2] for variable amplitude stresses subjected to BS4360 50B steel. The response of the steel to fatigue crack growth rate was found to be independent of specimen thickness and the prediction of crack growth was performed reasonably by linear summation using the Paris law. In their analysis, no significant improvement is achieved neither by considering crack closure effect nor to the choice of technique of cycle counting. A proposed method for fatigue lifetime prediction was made by Wang et al. [3] whereby aluminum alloy wheels was proposed to ensure their durability at the initial design stage. To simulate the rotary fatigue test, static load FEM model was built using ABAQUS. Therefore, the finite element model can achieve results consistent with that obtained from the actual static load test. The nominal stress method was used to predict the fatigue life of aluminum alloy wheels. In the nominal stress method, the fatigue life of aluminum wheels was predicted by using aluminum alloy wheel *S-N* curve and equivalent stress amplitude. Aluminum alloy wheel rotary fatigue bench test was conducted. The test result showed that the prediction of fatigue life was consistent with the physical test result. These results indicate that the fatigue life simulation can predict weakness area and is useful for improving aluminum alloy wheel. These results also indicate that integrating FEA and nominal stress method is a good and efficient method to predict aluminum alloy wheels fatigue life. Another attempt to increase the fatigue endurance limit and hence fatigue performance is due to Taylor [4] who conducted a study of evaluating a number of sinter-hardening materials based on MPIF standard grades and the effect that case carburizing had on developing beneficial residual compressive stresses in the surface with a resulting increase in fatigue endurance limit. The aim of his work was to improve the fatigue performance over traditional FLC and FLNC P/M sinter hardening grades. The results showed that there were two principle options to improve the fatigue performance of sinter-hardening steels. The first option required both a material and process change utilizing a silicon alloyed sinter hardening steel coupled with high temperature sintering. This option developed fatigue strength improvements of up to 30% over standard sinter-hardening grades. As an extension of the experimental work performed later, fatigue testing of a standard FLNC-4408 and Ancorloy MDCL showed the silicon-containing alloy had nearly a 30% improvement in fatigue life. As expected, the carburizing showed improvements over the standard sinter-hardening processing. Fatigue life improvements up to 50% over the standard FLNC-4408 were achieved by optimizing both the material and processing. Abrasive waterjet (AWJ) peening has been proposed by Arola et al. [5] as an applicable method of surface treatment for metal orthopedic devices. In this work, the influence of AWJ peening on the compressive residual stress, surface texture and fatigue strength of a stainless steel (AISI 304) and titanium (Ti6Al4V) alloy were studied. A design of experiments (DOE) and an analysis of variance (ANOVA) were used to identify the primary parameters contributing to the surface texture and magnitude of surface residual stress. The influence of AWJ peening on the fatigue strength of the metals was evaluated under fully reversed cyclic loading. It was found that AWJ peening results in compressive residual stress and is primarily influenced by the abrasive size and treatment pressure. Using the optimum treatment parameters for maximizing the residual stress, the endurance strength of Ti6Al4V was increased by 25%. When it comes to the extremely thin sheets or foils, an invaluable work of Hadrboletz et al. [6] may be noted. In the range of plate thickness from 20μm to 250μm, the LEFM and the subsequent formulas derived, becomes inapplicable due to the prevalence of plane stress state and extensive plastic yielding accompanying crack propagation due to fatigue failure. Metallic thin foils, subjected to fatigue loading caused by thermal fluctuations and mechanical vibrations, were examined. In their investigation, fatigue crack growth near threshold in the high cycle fatigue regime and associated fracture processes were studied. Freestanding rolled and electrodeposited Cu, Mo and Al foils of thickness from 20μm to 250 μm in different conditions had been tested in a special experimental setup. In a load shedding technique fatigue, threshold stress intensity factor values have been derived and compared with data of bulk material. Typical crack growth features were detected depending on thickness and grain sizes of the foils. Investigations of rolled, annealed and electrodeposited Cu foils of different grain sizes revealed that the so called size effect may be

observed if the ratio of the grain size to the foil thickness is close to or larger than unity and the constitutive length scale of the apparent plastic strain gradient is a considerable portion of the foil thickness. A size-effect was detected for fatigue crack growth data of rolled foils. Because the electrodeposited foils consist of a multilayered fine grain structure, no size effect is observed and the fatigue crack growth behavior is similar to bulk material. From the existing literature, it might be stated that the efforts made to extend fatigue life, were either undertaken to prolong the crack initiation stage or through delaying the crack propagation. It is believed that the fatigue life can be extended considerably by introducing multiple barriers against fatigue crack propagation in the material. Thus, the present work proposes a design, which relies on the concept of using a multilayered- rather than a bulk- structure of shafts and beams. An effort has also been made to predict fatigue life in order to verify the advantages of such proposed design.

3. Proposed Design of Beams

The proposed design of beams against fatigue is depicted in Figure 1. In order to make the design viable, a pretension thin metallic sheet or foil is wrapped around a core beam or mandrel until the final desired dimension is reached. An outer, so-called housing layer is introduced for purposes of protection and integrity. The housing layer can be made by depositing a suitable material. Moreover, the sheet can be bonded by an adhesive material, which may enhance arresting action of crack propagation via the boundaries of layers. This "layered design" is believed to have many advantages over the single or monolithic design; these are:

1. It provides multi-boundaries, which, act as barriers to crack propagation across the beam, and hence extend the fatigue life as will be shown later.
2. The pretension of the thin sheet prior to wrapping procedure sets longitudinal compressive stresses favorable in the presence of any crack existing or being initiated during the fluctuating loading of the beam.
3. The size of the core beam or mandrel can be chosen to serve as a final warning signal to the impending fast fracture of the component.
4. It is easier to produce crack-free surfaces with thin sheets or foils than with single or monolithic beams.

Although the manufacture of such beams is not yet presented, the following sections deal with the fatigue life prediction to assess the improvement achieved using the proposed design; a full description of the manufacture and experimentation of layered beam is currently processing.

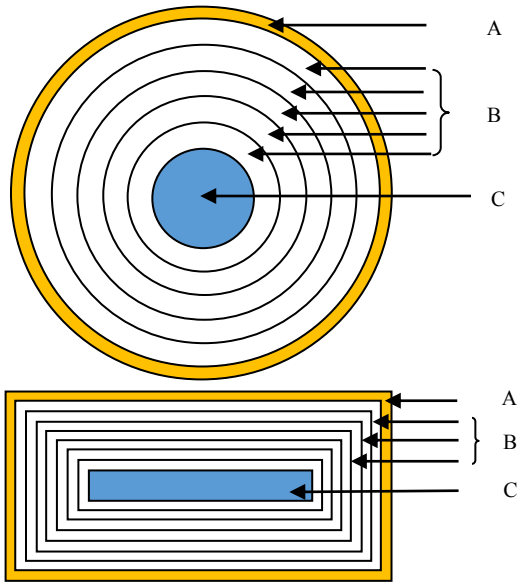

Figure 1: Schematic of proposed design of circular and rectangular beams: A: Housing layer, B: Thin metallic layers, C: Mandrel

4. Fatigue Life Prediction

The following analysis was generally simplified through several considerations concerning type and level of loading as well as some necessary assumptions made with justifications based on experimental observations. These are:

1. The beam is subjected to pure bending which fluctuates between M_{max} and M_{min}, so that $R = -1$, or $\sigma_{mean} = 0$ and such that $\Delta K > \Delta K_{th}$, where ΔK_{th} is the threshold value of the stress intensity factor range, ΔK.
2. The housing layer neither contributes to fatigue life of the layered section of the beam nor affects the mechanism of crack initiation in the outer layer underneath.
3. The failure mechanism of the layered beam starts when the housing layer is ruptured and the outer layer surface is exposed. At some point on the surface, a micro-crack is initiated by the action of either a defect, or the slip-band mechanism, or the reversal plastic deformation in the zone ahead of the crack. The crack will develop along the active slip plane aligned with the direction of maximum shear within the component, i.e. at 45^0 to the maximum tensile stress (StageI). This is followed by StageII in which the crack is normal to the maximum principal tensile stress and the crack grows from a predetermined initial value, a_i to a critical final value, a_f. The crack propagates both radially through the thickness and circumferentially along the perimeter just in the same way as in a single

monolithic shaft except that the radial component of the crack is being arrested at the interface with the next adjacent layer. The circumferential component continues until it reaches its critical value, a_f, i.e, K_C is approached. When K_C is exceeded, a final fast fracture of the layer occurs. This final stage (StageIII) is presently neglected. When the surface of the next layer is exposed, the same sequence of events will be repeated in the rest of the layers down to the inner layer until the surface of the mandrel is reached where the life of the component is considered to come to its end.

4. Although StageI has never been quantified before, a rough estimate for the number of cycles was made because of its important role in the proposed design. The number of cycles, endured during StageI (NI) was calculated from the instance when the crack grows from an already-existing microcrack of size a_0 to some macrocrack of size a_i as shown in Figure 2.

5. Although StageII was presumed to start when the crack grows from a predetermined initial value, a_i to a critical final value, a_f , the present analysis has been made conservative by assuming the second stage terminates when the crack length reaches either a_f or the thickness of the layer t whichever the least.

6. Although the amplitude of the stress intensity factor ΔK is used to express the crack growth in brittle materials or those with well-contained plasticity in which a plane strain state of stress is dominating, nevertheless a recent work by Hadrboletz et al.[6] has related the experimental observations of crack growth of Cu foils with ΔK and similar trends to that of the well-known Paris-Erdogan law, $da/dN = C(\Delta K)^m$ were observed.

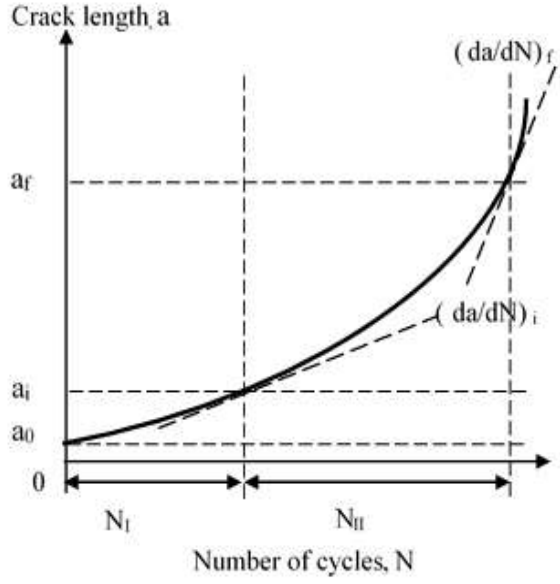

Figure 2: Fatigue crack during life cycles

Following on the above, the fatigue life of a round beam of outer radius R, constructed by wrapping a thin layer around a mandrel shaft of radius r_m , was estimated hereafter.

As mentioned earlier, the mandrel size may be selected to guard against failure when the stress approaches the ultimate tensile strength, i.e.:

$$\sigma_u = \frac{M_{max}}{Z} = \frac{4M_{max}}{\pi r_m^3} \quad (1)$$

from which:

$$r_m = \sqrt[3]{\frac{4M_{max}}{\pi\sigma_u}} \quad (2)$$

The number of layers, M which can be used is, thus:

$$M = \frac{R - r_m}{t} \quad (3)$$

where t is the thickness of the layer.

The range of maximum stress intensity factor is:

$$\Delta K_{max} = \alpha\, \Delta\sigma_{max}\sqrt{\pi a} \quad (4)$$

where α is a correcting factor which refers to the type of loading and crack configuration and taken as unity for the given configuration, and:

$$\Delta\sigma_{max} = \frac{2M_{max}}{Z} = \frac{8M_{max}}{\pi r^3} \quad (5)$$

where r is the radial distance of a layer from the neutral axis of the beam, i.e.:

$$r = R - nt \quad (6)$$

where $n = 0, 1, 2, 3, \ldots, M-1$

The number of cycles endured during StageI can be deduced from:

$$\int_0^{N_I} dN = \int_{a_0}^{a_i} \frac{da}{C(\Delta K_{max})^m} \quad (7)$$

where C and m are constant coefficients of the layer material. Therefore:

$$N_I = \frac{2}{C(m-2)} \cdot \left(\frac{r^3\sqrt{\pi}}{8M_{max}}\right)^m \left(\frac{1}{\sqrt{{a_0}^{m-2}}} - \frac{1}{\sqrt{{a_i}^{m-2}}}\right) \quad (8)$$

Likewise, the number of cycles endured during StageII can be deduced from:

$$\int_0^{N_{II}} dN = \int_{a_i}^{d} \frac{da}{C(\Delta K_{max})^m} \quad (9)$$

Or:

$$N_{II} = \frac{2}{C(m-2)} \cdot \left(\frac{r^3\sqrt{\pi}}{8M_{max}}\right)^m \left(\frac{1}{\sqrt{{a_i}^{m-2}}} - \frac{1}{\sqrt{d^{m-2}}}\right) \quad (10)$$

where d is the value of either a_f or the thickness of the layer t, whichever the least.

The critical value of the crack length a_f was evaluated when K approaches K_C, i.e.:

$$K_C = \sigma_{max}\sqrt{\pi a_f} \quad (11)$$

from which:

$$a_f = \pi\left(\frac{r^3 K_C}{4M_{max}}\right)^2 \quad (12)$$

It should be noted that, Eq.(12) and Eq.(6) imply that t is always smaller than a_f so that d in Eq.(10) can be safely replaced by t. Combining Eqs.(8 and 10), the total fatigue life of a layer was predicted as:

$$N_n = N_I + N_{II} = \frac{2}{C(m-2)} \cdot \left(\frac{r^3\sqrt{\pi}}{8M_{max}}\right)^m \left(\frac{1}{\sqrt{{a_0}^{m-2}}} - \frac{1}{\sqrt{t^{m-2}}}\right) \quad (13)$$

Finally, the total number of cycles endured by a multilayered component is:

$$N_T = \sum_{n=0}^{M-1} N_n \quad (14)$$

As a special and reference case, the total number of cycles endured by a single monolithic component can be deduced from Eq.(14) with M=1. The improvement attained of fatigue life due to layering the beam was conventionally determined as:

$$Improvement\% = \frac{N_{T(M)} - N_{T(M=1)}}{N_{T(M=1)}} \times 100\% \quad (15)$$

5. Results and Discussion

It must be borne in mind that the present design relies on a theoretical, yet feasible concept of introducing barriers in front of the crack commonly growing across the section of components subject to fatigue loading. In doing so, the crack initiated in the first stage propagates during the second stage through the entire of layer thickness. At this point, the crack will be confronted by the discontinuity in the medium of solid material and will no longer be able to grow further. In other words, the crack will be terminated and a new crack has to be initiated during the next stage. The result is the advantageous repetition of the first stage although the second stage will be interrupted. In order to explain the sequence of events described above, a plain and simple analysis was made to quantify fatigue life during the two stages for both the so-called monolithic and layered versions of beams. The aim is to determine the improvement in fatigue life of a layered beam, if any, compared with the monolithic beam. A numerical example is thus made in which the physical and mechanical properties are selected as:

$R = 10\,mm$; $\sigma_u = 800\,MPa$
$M_{max} = 100\,N.m$; $C = 10^{-11}$
$m = 3$; $K_C = 30\,MPa\sqrt{m}$
$a_0 = 10^{-3}mm$; $a_i = 0.1mm$

Although these figures do not refer to a certain material, nevertheless they are within the data cited in many books, see for example Ref. [7]. Introducing these figures in the various equations of the present analysis, the fatigue life for each layer during both stages together with the total number of cycles endured by the beam are listed in Table 1. For convenience, the results were also presented in Figures 3, 4, and 5. Referring to Fig.3, the so-called incubation period or StageI- N_I in short- is repeated in each layer and for all types of layered beams, i.e. for different values of (M). Moreover, the cycles endured for (n=0) are the same for all types of beams because the crack can propagate to the full value of (a_i) before confronting the boundary of the next layer, i.e. because a_i is less than the layer thickness t; Should the number of layers is increased so that the above relation is reversed, the conclusion of constant N_I for all values of (M) will be no longer

valid. Whether N_I is constant for all external layers (n=0) or not, the value of N_I for the layered beams (n≠0) is increased as the beam cross section is more laminated, and the more number of layers are used, the higher number N_I and hence the improvement is attained. It must be also pointed out that the additional cycles attained for a given layered beam are continually decreasing, see the case (M=7) for example.

Table 1: Number of fatigue cycles endured during stages I & II for layered beam.

M	t(mm)	n	N_I (cycle)	N_{II} (cycle)	N_n (cycle)	N_T (cycle)	Improv-ement,%
1	4.581	0	1 957 500	185 430	2 142 930	2 142 930	---
2	2.291	0	1 957 500	172 151	2 129 651	2 332 294	9
		1	186 259	16 384	202 643		
3	1.527	0	1 957 500	161 895	2 119 395	2 674 038	25
		1	439 190	36 307	475 497		
		2	73 103	6 043	79 146		
4	1.145	0	1 957 500	153 363	2 110 863	3 056 185	43
		1	651 915	51 070	702 985		
		2	180 900	14 594	195 494		
		3	43 438	3 405	46 843		
5	0.916	0	1 957 500	145 792	2 103 292	3 471 874	62
		1	821 248	61 165	882 413		
		2	313 988	23 387	337 375		
		3	106 991	7 969	114 960		
		4	31 489	2 345	33 834		
6	0.764	0	1 957 500	138 965	2 096 465	3 890 845	82
		1	954 525	67 772	1 022 297		
		2	437 327	31 050	468 377		
		3	186 042	13 208	199 250		
		4	72 348	5 137	77 485		
		5	25 183	1 788	26 971		
7	0.654	0	1 957 500	132 645	2 090 145	4 317464	102
		1	1 061 888	71 961	1 133 849		
		2	550 909	37 333	588 242		
		3	271 428	18 394	289 822		
		4	125 884	8 531	134 415		
		5	54 340	3 682	58 022		
		6	21 511	1 458	22 969		

This steady reduction in N_I is essentially due to the higher stress induced in surface fibers resulting from the reduced modulus of the remaining section, see Eq.(8).Consequently and in an overall manner, it can be stated that the use of more layers will enhance fatigue life through extending the incubation period, or StageI. The story in Fig.4 is somewhat different in that the number of cycles endured during StageII- N_{II} in short –is decreasing as the beam section is more laminated, in view of the reduced thickness of the layer, see Eq.(10); more reduction in N_{II} is due to reduction in section modulus. Recalling the argument of conservative-analysis assumption made earlier, the thickness of layer t has been chosen instead of a_f as the final limit of crack length propagating during the second stage; In other words, the second stage has been made shorter since t had been proved to be always less than a_f. Even if the latter was chosen in the analysis, the value of N_{II} will still decrease as a result of reduction in the a_f value, see Eq.(12). On the other hand, the cross section lamination will have a counteracting effect in that there is additional and increasing gain in N_{II} as a result of lamination. For example the additional N_{II} for the secondlayer will compensate the reduction and seems that there is a critical case of faster compensation at M=5. The increasing trend in the additional layers used is attributed to the greater influence of stress reduction relative to the reduction in layer thickness. In addition, the additional contribution to fatigue life is less for the layer closer to the mandrel shaft in a direct

result of layer thickness reduction. Once again, the total contribution of layers to the second stage of fatigue life seems to increase more and more by fine lamination rather than coarse lamination.Finally when the number of cycles endured in both stages are added up together, the result would be as shown in Fig.5. For the outer layer of all types of layered beams (n=0), the total number of cycles endured N_T is shown to be slightly decreasing by the effect of increasing number of layers. In turn, the second layer soon compensates that loss, and in fact, the improvement is huge and instant. As the beam is more laminated, the improvement will be enhanced rapidly and attains a value as high as 102% by only M=7 laminations. Thus, the improvement attained by the present design is dramatic when compared with previous attempts like those of Taylor [4] who reported an improvement of 30-50% and Arola et al. [5] of 25%. The same justifications of Figs.3 and 4 are true for Figure 5 regarding both the increased extent of contribution per layer in beams, and the reduced extent of contribution per layers in a beam.

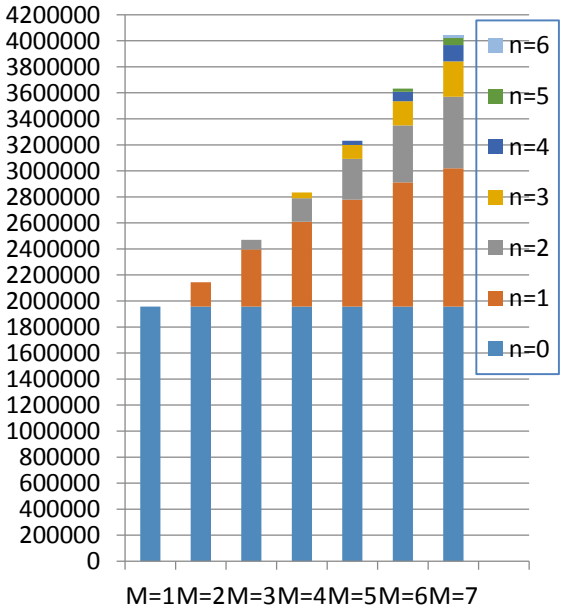

Figure 3: Number of cycles endured in the first stage (N_I) for different number of layers (M).

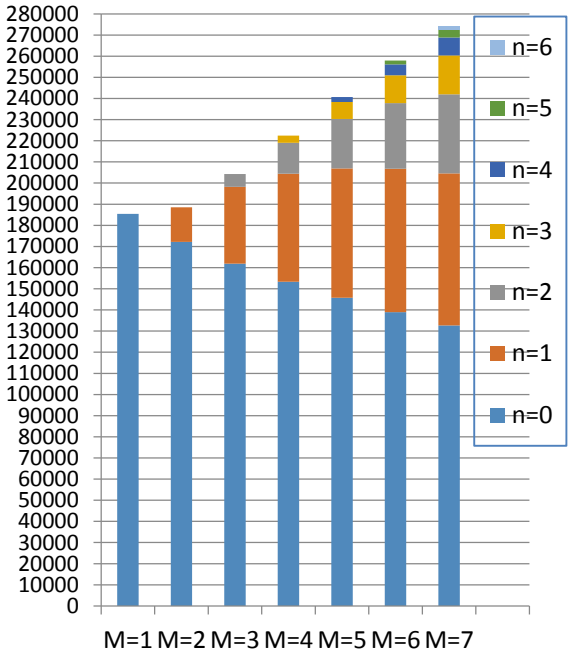

Figure 4: Number of cycles endured in the second stage (N_{II}) for different number of layers (M).

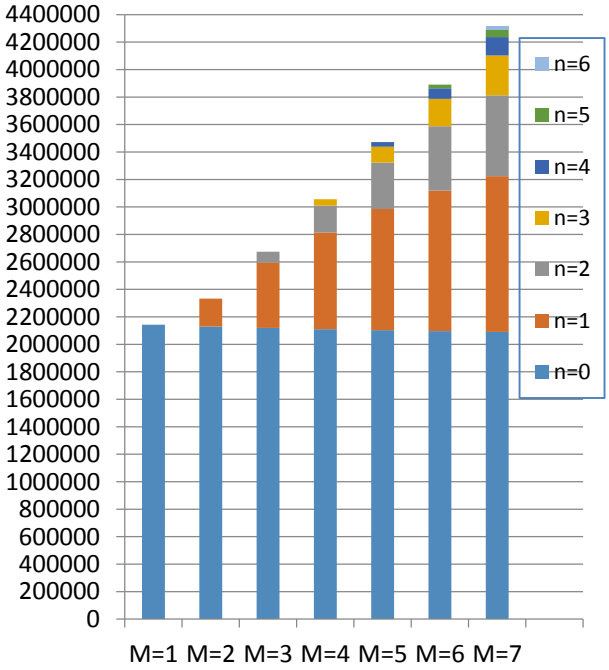

Figure 5: Total number of cycles endured (N_T) for different number of layers (M).

6. Conclusions

The main conclusions, which can be drawn out of the present work, were summarized as:

1. Despite the huge efforts so far made to understand and/or defeat the fatigue phenomena, there are still many occasions in which mechanical components fail catastrophically. These efforts are mainly aimed towards innovative design to enhance fatigue characteristics and life, or elaborations to achieve easier nondestructive prediction of fatigue life.

2. The well-known Paris-Erdogan formula was proved capable of theoretically predicting fatigue life of wide range of materials, ductile or brittle, thick or thin, provided that the governing constants are well evaluated through experimentation.
3. The present proposed design was shown to enhance fatigue properties through laminating the cross section of the component; Barriers in front of a propagating crack is deliberately included by lamination.
4. Spectacular levels of improvement in the fatigue life of up to 102% were achieved by replacing the monolithic type by only seven laminates.
5. The present analysis was proved efficient in verifying the anticipated improvement acquired by the proposed design of laminated beams.

References

[1] O. Kovarika, P. Hausilda, J. Siegla, J. Matejicekb, and V. Davydovc, "Fatigue life of layered metallic and ceramic plasma sprayed coatings," 20th European Conference on Fracture (ECF20) Procedia Materials Science 3, pp.586 – 591, 2014.

[2] N.A Fleck and R.A. Smith, "Fatigue life prediction of a structural steel under service loading," International Journal of Fatigue, Vol. 6, No. 4, pp.203-210, 1984.

[3] L. Wang, Y. Chen, C. Wang, and Q. Wang, "Fatigue Life Analysis of Aluminum Wheels by Simulation of Rotary Fatigue Test," Journal of Mechanical Engineering, Vol. 57, No. 1, pp. 31-39, 2011.

[4] F. Hanejko and A. Taylor, "Advanced Sintering Materials and Practices," Advances in Powder Metallurgy and Particulate Materials, Part 13, pp 13-29, Metal Powder Industries Federation, Princeton, NJ, 2002.

[5] D. Arola, A. E. Alade, and W. Weber, "Improving fatigue strength of metals using abrasive waterjet peening," Machining Science and Technology, Vol. 10, pp.197–218, 2006.

[6] A. Hadrboletz, B. Weiss and G. Khatibi, "Fatigue and fracture properties of thin metallic foils," International Journal of Fracture Vol. 107, pp.307–327, 2001.

[7] E.J. Hearn, "Mechanics of Materials 2," Butterworth-Heinemann, Third Edition, Oxford, 1997.